

pH-Controlled Assemblies of Dimethyltin-Functionalized 9-Tungstophosphates with Guanidinium as Structure-Directing Cation

Santiago Reinoso,^[a,b] Bassem S. Bassil,^[a] Maria Barsukova,^[a] and Ulrich Kortz*^[a]

Keywords: Polyoxometalates / Organotin compounds / Hybrid materials / Template synthesis / Tungsten / Tin

Aqueous reaction of $(\text{CH}_3)_2\text{SnCl}_2$ with $\text{Na}_9[\text{A-}\alpha\text{-PW}_9\text{O}_{34}]$ in a 3:1 ratio with $[\text{C}(\text{NH}_2)_3]^+$ as structure-directing agent resulted in three distinct assemblies of dimethyltin-functionalized tungstophosphates depending on the pH: $\{[(\text{CH}_3)_2\text{Sn}(\text{H}_2\text{O})]\{(\text{CH}_3)_2\text{Sn}(\text{A-}\alpha\text{-PW}_9\text{O}_{34})\}^{5-}\}$ (**1**) at pH = 4.5; $\{[(\text{CH}_3)_2\text{Sn}(\text{H}_2\text{O})_2]\{(\text{CH}_3)_2\text{Sn}(\text{H}_2\text{O})\}_2(\text{A-}\alpha\text{-PW}_9\text{O}_{34})\}^{3-}\}$ (**2**) at pH = 3.0; and $\{[(\text{CH}_3)_2\text{Sn}(\text{H}_2\text{O})]_3(\text{A-}\alpha\text{-PW}_9\text{O}_{34})\}^{3-}\}$ (**3**) at pH = 2.0. All three compounds have been characterized in the solid-state by elemental and thermal analyses, infrared spectroscopy and single-crystal X-ray diffraction. The $[\text{A-}\alpha\text{-PW}_9\text{O}_{34}]^{9-}$

trilacunary fragments have three $\{(\text{CH}_3)_2\text{Sn}\}^{2+}$ groups anchored on the vacant sites via two Sn–O(W) bonds each and they are linked into guanidinium-templated, extended architectures with dimensionalities increasing with the acidity of the reaction media. The structure of **1** consists of a 1-dimensional arrangement of alternating $[\text{A-}\alpha\text{-PW}_9\text{O}_{34}]^{9-}$ subunits and *trans*-($\text{CH}_3)_2\text{SnO}_4$ bridging moieties, whereas compounds **2** and **3** are 2- and 3-dimensional assemblies, respectively, of monomeric $\{[(\text{CH}_3)_2\text{Sn}]_3(\text{A-}\alpha\text{-PW}_9\text{O}_{34})\}^{3-}$ building blocks connected via weak intermolecular Sn–O=W bridges.

Introduction

Polyoxometalates (POMs) are metal-oxygen clusters with a remarkable compositional and structural variety.^[1] Derivatization of POMs via covalent attachment of organic/organometallic moieties to the metal-oxo framework allows for enhancement and fine-tuning of the acid-base, redox, and/or electronic properties, therefore affording hybrid species with potential applications in diverse fields (e.g. catalysis, materials science, medicine). Organotin groups are suitable candidates for systematic POM functionalizations because the Sn–C bond is reasonably stable toward hydrolysis, and the size of Sn^{IV} is apt to substitute addenda metal centres in POM skeletons. Thus, several monomeric or dimeric POMs composed of lacunary Keggin or Wells–Dawson polytungstates with firmly anchored mono-organotin fragments have been reported.^[2] In addition, our studies on the ability of the $\{(\text{CH}_3)_2\text{Sn}\}^{2+}$ group as linker of polytungstates and -molybdates have led to several unprecedented POM architectures over the last few years, including monomeric to dodecameric discrete assemblies of lacunary heteropolytungstates and extended polyanion-based materials.^[3]

Among several factors (e.g., pH and temperature), the features of the countercation constitute a key factor in the formation of several POMs, and therefore, studying the structure-directing role of the countercation constitutes an important research objective to allow for a rational design of tailored POM assemblies. In this context, the group of Cronin has investigated the templating effect of some organo-ammonium cations in the construction of novel POM frameworks.^[4] Moreover, our group found that $[\text{C}(\text{NH}_2)_3]^+$ appears to be a selective crystallizing agent for dimethyltin-containing POMs that are present in solution as minor species or cannot be isolated by using other cations (e.g., alkali ions).^[3f,3i] Recently, we reported the first 3-dimensional architecture of organotin-functionalized POMs formed by tetrahedrally arranged $\{(\text{CH}_3)_2\text{Sn}\}_3(\text{A-}\alpha\text{-XW}_9\text{O}_{34})$ building blocks ($\text{X} = \text{P}^{\text{V}}, \text{As}^{\text{V}}, \text{Si}^{\text{IV}}$) connected via weak intermolecular Sn–O=W bridges.^[3j] This type of assembly is templated by $[\text{C}(\text{NH}_2)_3]^+$ as a result of its trigonal-planar geometry and hydrogen bonding ability regardless of the size or charge of the heteroatom X. The fact that dodecameric, discrete POMs are formed under similar reaction conditions^[3c] in the presence of Cs^+ ions suggests that the $\{(\text{CH}_3)_2\text{Sn}\}_3(\text{A-}\alpha\text{-XW}_9\text{O}_{34})$ monomers could be used as versatile tailor-designed building blocks in the crystal engineering of new materials. Therefore, we decided to investigate the structure-directing role of organo-ammonium cations in the formation of supramolecular aggregates of $\{(\text{CH}_3)_2\text{Sn}\}_3(\text{A-}\alpha\text{-XW}_9\text{O}_{34})$ monomeric species.

Here we report on the influence of the pH in the dimensionality of $[\text{C}(\text{NH}_2)_3]^+$ templated assemblies of dimethyltin-containing 9-tungstophosphates. This work resulted in three distinct compounds, obtained from reaction of the

[a] School of Engineering and Science, Jacobs University
P. O. Box 750561, 28725 Bremen, Germany
E-mail: u.kortz@jacobs-university.de

[b] Instituto de Ciencia Molecular (ICMol), Universidad de Valencia
Polígono de La Coma s/n, 46980 Paterna, Valencia, Spain

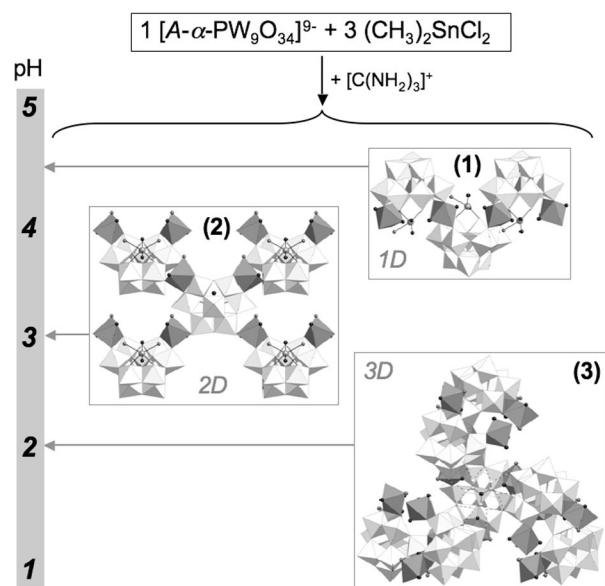
Supporting information for this article is available on the WWW under <http://dx.doi.org/10.1002/ejic.201000185>.

$\{(\text{CH}_3)_2\text{Sn}\}^{2+}$ electrophile with the trilacunary $[\text{A-}\alpha\text{-PW}_9\text{O}_{34}]^{9-}$ Keggin polyanion in water at different pH values: $\text{Na}_{0.5}[\text{C}(\text{NH}_2)_3]_{4.5}\{[(\text{CH}_3)_2\text{Sn}(\text{H}_2\text{O})]\{(\text{CH}_3)_2\text{Sn}\}(\text{A-}\alpha\text{-PW}_9\text{O}_{34})\}\cdot 8.5\text{H}_2\text{O}$ (**1**) at pH = 4.5; $[\text{C}(\text{NH}_2)_3]_3\{[(\text{CH}_3)_2\text{Sn}(\text{H}_2\text{O})]\{(\text{CH}_3)_2\text{Sn}(\text{H}_2\text{O})\}_2(\text{A-}\alpha\text{-PW}_9\text{O}_{34})\}\cdot 8\text{H}_2\text{O}$ (**2**) at pH = 3.0; and $\text{Na}[\text{C}(\text{NH}_2)_3]_2\{[(\text{CH}_3)_2\text{Sn}(\text{H}_2\text{O})]\{(\text{CH}_3)_2\text{Sn}(\text{H}_2\text{O})\}_3(\text{A-}\alpha\text{-PW}_9\text{O}_{34})\}\cdot 9\text{H}_2\text{O}$ (**3**) at pH = 2.0.

Results and Discussion

Synthesis

Recently, we demonstrated that the $[\text{C}(\text{NH}_2)_3]^+$ cation can be used as a structure-directing agent to construct supramolecular arrangements of monomeric $\{(\text{CH}_3)_2\text{Sn}\}_3(\text{A-}\alpha\text{-XW}_9\text{O}_{34})$ building-blocks. This cation acts as a template for a certain architecture regardless of the charge and size of the heteroatom X, resulting in the first 3-dimensional assemblies of organotin functionalized heteropolytungstates.^[3j] Considering the versatility of these monomers to assemble via weak intermolecular Sn-O-W bridges, we decided to investigate the influence of the pH on the templating ability of $[\text{C}(\text{NH}_2)_3]^+$. Thus, we reacted the selected $[\text{A-}\alpha\text{-PW}_9\text{O}_{34}]^{9-}$ precursor with 3 equivalents of $\{(\text{CH}_3)_2\text{Sn}\}^{2+}$ in hot water with the pH value as the single variable. The initial pH of the reaction was 4.5 and the 1-dimensional hybrid $\{[(\text{CH}_3)_2\text{Sn}(\text{H}_2\text{O})]\{(\text{CH}_3)_2\text{Sn}\}(\text{A-}\alpha\text{-PW}_9\text{O}_{34})\}^{5-}$ polyanion was isolated as **1** at such moderately acidic conditions. Addition of a minimum fraction of acid suddenly lowered the pH to about 3, at which the monomeric $[\{(\text{CH}_3)_2\text{Sn}\}_3(\text{A-}\alpha\text{-PW}_9\text{O}_{34})]^{3-}$ species was formed. Guanidinium directs the formation of two different supramolecular architectures of this monomeric building block, which were obtained separately as a function of the medium acidity: the 2-dimensional **2** at pH = 3.0 and the 3-dimensional **3** at pH = 2.0 (Scheme 1).



Scheme 1. Synthetic procedure for compounds 1–3.

Infrared Spectroscopy

The infrared spectra (IR) of **1–3** are reminiscent of the precursor with significant changes in some band positions and intensities, indicating retention of the $[\text{A-}\alpha\text{-PW}_9\text{O}_{34}]^{9-}$ fragment upon functionalization (Figure S1). The $\{(\text{CH}_3)_2\text{Sn}\}^{2+}$ moieties are unequivocally identified by weak peaks in the range 1190–1210 cm^{-1} assigned to the $\delta_s(\text{CH}_3)$ vibration in methyltin derivatives.^[5] Compounds **1–3** can be clearly distinguished by IR despite being composed of similar building blocks, and consequently, showing closely related spectra. The spectrum of **1** displays two signals originating from the $\nu_{\text{as}}(\text{P-O})$ mode (a pair of strong peaks and a single medium intensity peak at about 1070 and 1005 cm^{-1}), a group of three signals related to the $\nu_{\text{as}}(\text{W-O}_i)$ vibration with intensities decreasing to lower wavenumbers (two strong peaks and a shoulder at about 935, 905, and 890 cm^{-1}), four strong to very strong bands in the range 835–670 cm^{-1} assigned to the $\nu_{\text{as}}(\text{W-O-W})$ mode, and a medium peak at about 520 cm^{-1} corresponding to bending vibrations. For **2** and **3**, splitting of the $\nu_{\text{as}}(\text{P-O})$ signal is not observed and the medium $\nu_{\text{as}}(\text{P-O})$ peak and the two strong $\nu_{\text{as}}(\text{W-O}_i)$ peaks are 10–15 cm^{-1} blueshifted, leading to resolution of the $\nu_{\text{as}}(\text{W-O}_i)$ shoulder in a separate signal of medium intensity at about 890 and 900 cm^{-1} for **2** and **3**, respectively. In addition, the $\nu_{\text{as}}(\text{W-O-W})$ band at lower wavenumbers is masked by broadening of the signals in this region, resulting in a pattern of three bands in the range 835–720 cm^{-1} where the central one in **3** is redshifted for ca. 20 cm^{-1} .

Thermal Analysis

The thermal analyses of **1–3** show similar trends (Figure S2). Mass loss starts at room temperature with a dehydration step below ca. 180 °C (**1**, 170; **2**, 190; **3**, 190 °C) involving the release of 9.5 and 12 water molecules for **1** and **3**, respectively [% calcd. (found): **1**, 5.74 (5.66); **3**, 7.12 (7.25)]. In the case of **2**, only 11 of the 12 water molecules observed by X-ray crystallography could be determined [% calcd. (found): 6.49 (6.54)]. Dehydration is immediately followed by the release of the $[\text{C}(\text{NH}_2)_3]^+$ cations together with the loss of the methyl groups in a second mass loss step below 420, 435, and 445 °C for **1–3**, respectively [% calcd. (found): **1**, 11.55 (11.61); **2**, 8.86 (8.31); **3**, 6.93 (7.41)]. After a narrow stability range, the resulting metal-oxo frameworks undergo final decomposition above 475 (**1**), 515 (**2**), and 540 °C (**3**).

Structure of 1

The polymeric $[\{(\text{CH}_3)_2\text{Sn}(\text{H}_2\text{O})\}\{(\text{CH}_3)_2\text{Sn}\}(\text{A-}\alpha\text{-PW}_9\text{O}_{34})]^{5-}$ polyanion in **1** consists of alternating trilacunary $[\text{A-}\alpha\text{-PW}_9\text{O}_{34}]^{9-}$ subunits and $\{(\text{CH}_3)_2\text{Sn}\}^{2+}$ bridging moieties linked in a 1-dimensional assembly (Figure 1). These subunits, derived from the parent $[\text{A-}\alpha\text{-PW}_{12}\text{O}_{40}]^{3-}$ Keggin ion by removal of three corner-sharing WO_6 octahe-

dra, are decorated by additional $\{(CH_3)_2Sn\}^{2+}$ pendant groups, in such a way that each trilacunary fragment is connected to three $\{(CH_3)_2Sn\}^{2+}$ electrophiles grafted on the vacant sites through two Sn–O(W) bonds. Two adjacent $[A-\alpha-PW_9O_{34}]^{9-}$ subunits are linked by equatorial coordination of one $\{(CH_3)_2Sn\}^{2+}$ bridging moiety (Sn1) to two pairs of edge-sharing WO_6 octahedra with a regular Sn–O bonding in the range 2.174(11)–2.271(11) Å. The octahedral $(CH_3)_2SnO_4$ geometry is completed by the methyl groups in the axial positions with a relative *trans* arrangement. In contrast, the Sn centers in the pendant groups (Sn2) are penta-coordinate and exhibit a highly distorted $(CH_3)_2SnO_3$ geometry which is best described as trigonal-bipyramidal. The equatorial plane is composed of one O atom from the third edge-shared $\{W_2O_{10}\}$ dimer and the two methyl groups, which therefore display a relative *cis* arrangement. Another O atom of the $\{W_2O_{10}\}$ dimer and the O2Sn oxo ligand, assigned as a water molecule by bond valence sum (BVS) calculations,^[6] occupy the axial positions. All the Sn–O bonds are short, with the exception of the long Sn–O2Sn bond, in agreement with our previous polytungstates containing independent *cis*– $(CH_3)_2SnO_3$ groups (Table 1).^[3f,3i]

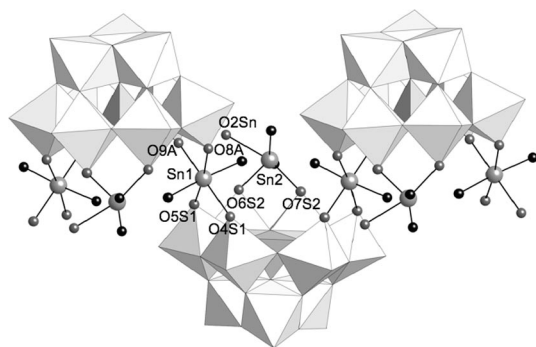


Figure 1. Polyhedral/ball-and-stick representation of the 1-dimensional polyanion $[\{ (CH_3)_2Sn(H_2O) \} \{ (CH_3)_2Sn \} (A-\alpha-PW_9O_{34})]^{5-}$ in **1** with atom labeling (hydrogen atoms omitted for clarity). Color code: WO_6 octahedra, white; PO_4 tetrahedra, light grey; Sn, grey; C, black; O, dark grey.

The zigzagging chains in **1** run along the *c* axis with some of the $[C(NH_2)_3]^+$ cations embedded in the space delimited by three consecutive $[A-\alpha-PW_9O_{34}]^{9-}$ subunits (Figure 2). These cations template the shape of the hybrid 1-dimensional assembly by determining the zigzagging angle through twelve $N-H\cdots O_{POM}$ contacts that hold alternating trilacunary fragments together. The chains are arranged in layers parallel to the *ac* and *bc* planes placed at $a = b = 1/4$ and $3/4$, in such a way that each polymeric polyanion is linked to the four nearest, 90° rotated neighbours through

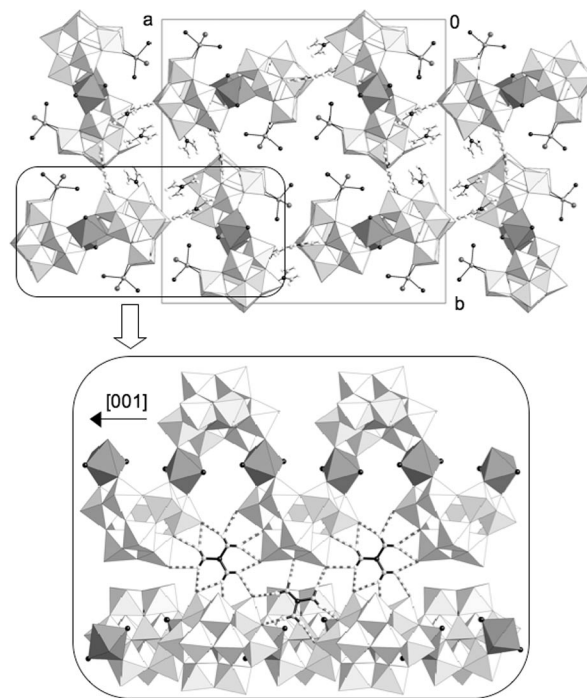


Figure 2. View of the crystal packing of **1** along the *c* axis (top) with a detail of the $N-H\cdots O_{POM}$ hydrogen-bonding network (dashed lines) between two adjacent polyanions (bottom, Sn2 groups not shown). Color code: same as Figure 1. Bridging Sn1 moieties represented as polyhedra to highlight the backbone of the zigzagging chains. Hydrogen atoms omitted for clarity.

Table 1. Selected bond lengths [Å] for the tin atoms in **1**–**3**.^[a]

1		2		3 ^[3]	
Bridging moieties					
Sn1–C1S1	2.106(19)	Sn1–C1S1	2.082(12)	Sn–C2	2.072(18)
Sn1–C2S1	2.135(17)	Sn1–C2S1	2.112(13)	Sn–C1	2.114(16)
Sn1–O9A ⁱ	2.174(11)	Sn1–O2S1	2.058(8)	Sn–O1S	2.078(11)
Sn1–O5S1	2.191(11)	Sn1–O1S1	2.102(8)	Sn–O2S	2.154(11)
Sn1–O8A ⁱ	2.253(12)	Sn1–O1Sn	2.398(9)	Sn–O1Sn	2.325(12)
Sn1–O4S1	2.271(11)	Sn1–O5T ⁱⁱ	2.706(8)	Sn–O2T	2.483(11)
Pendant groups					
Sn2–C2S2	2.02(3)	Sn2–C2S2	2.070(17)		
Sn2–C1S2	2.09(3)	Sn2–C1S2	2.10(2)		
Sn2–O6S2	2.063(13)	Sn2–O5S2	2.149(8)		
Sn2–O7S2	2.063(14)	Sn2–O5S2 ⁱⁱⁱ	2.149(8)		
Sn2–O2Sn	2.35(3)	Sn2–O2Sn	2.457(11)		
		Sn2–O2Sn ⁱⁱⁱ	2.457(11)		

[a] Symmetry codes, i: $1/2 - x, 1/2 - y, 1/2 + z$; ii: $1/2 - x, 1 - y, 1/2 + z$; iii: $x, 3/2 - y, z$.

an extended N–H⋯O_{POM} hydrogen bonding network involving almost all terminal and bridging O atoms with the exception of those coordinated to Sn centers or belonging to the edge-shared {W₂O₁₀} dimer onto which the pendant Sn2 group is anchored. This connectivity results in a 3-dimensional open-framework, displaying square-shaped hydrophobic channels, parallel to the [001] direction where the pendant groups are hosted.

Structures of 2 and 3

The crystal structures of **2** and **3** are extended assemblies of monomeric $[(CH_3)_2Sn\{3(A-\alpha-PW_9O_{34})\}]^{3-}$ building blocks, composed of three $\{(CH_3)_2Sn\}^{2+}$ electrophiles anchored via two Sn–O(W) bonds each on the vacant sites of a $[A-\alpha-PW_9O_{34}]^{9-}$ fragment. The geometry of the Sn atoms is highly distorted octahedral (CH₃)₂SnO₄ with the axial positions occupied by the methyl groups in a relative *trans* arrangement. In the case of **2**, two of the $\{(CH_3)_2Sn\}^{2+}$ electrophiles (Sn1) act as bridging moieties, whereas the remaining one (Sn2) constitutes a pendant group in analogy with the structure of **1** (Figure 3). The equatorial plane of the Sn1 atom is formed by two O atoms of an edge-shared {W₂O₁₀} dimer, one water molecule (O1Sn), and one terminal O atom belonging to the {W₆O₂₇} belt of a neighbouring monomeric unit (O5T). Unlike for **1**, this results in an irregular Sn–O bonding with two short bonds, a long Sn1–O1Sn bond and a very long Sn1–O5T bond, leading to a pattern analogous to other polytungstates containing *trans*-(CH₃)₂SnO₄ moieties (Table 1).^[3] On the other hand, the equatorial bonding of the Sn2 centers is defined by two short Sn–O bonds with a pair of edge-sharing WO₆ octahedra and two long bonds to water molecules (O2Sn). Diprotonation of the O1Sn and O2Sn oxo ligands is confirmed by BVS calculations.^[6]

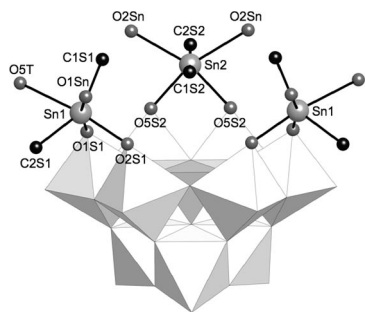


Figure 3. Polyhedral/ball-and-stick representation of the building block $[(CH_3)_2Sn(H_2O)_2]\{(CH_3)_2Sn(H_2O)\}_2(A-\alpha-PW_9O_{34})]^{3-}$ in **2** with atom labeling (hydrogen atoms omitted for clarity). Color code: same as Figure 1.

The crystal packing of **2** consists of 2-dimensional arrangements of $[(CH_3)_2Sn\{3(A-\alpha-PW_9O_{34})\}]^{3-}$ monomers parallel to the *bc* plane (Figure 4). Each building block is connected to the four nearest by four Sn1 bridging moieties, and more specifically, through four weak Sn–O=W inter-

molecular bridges involving the terminal atoms of the edge-shared {W₂O₁₀} dimers onto which the Sn2 pendant groups are grafted (W5/W5'). This assembly displays intralamellar spaces delimited by four adjacent, interconnected building blocks where groups of three stacked $[C(NH_2)_3]^+$ cations are buried. The latter stabilize the polyanion association by holding the four building blocks together through an intricate network of N–H⋯O hydrogen bonds with the W5/W5' containing tetrameric face of one monomer and the {W₆O₂₇} belts and/or O1Sn water molecules of the remaining three monomers. This type of connectivity leads to corrugated hybrid layers that pack along the *a* axis with the pendant Sn2 groups pointing to the interlamellar space, in such a way that the O2Sn water molecules are further involved in O–H⋯O_{POM} hydrogen bonding between adjacent layers.

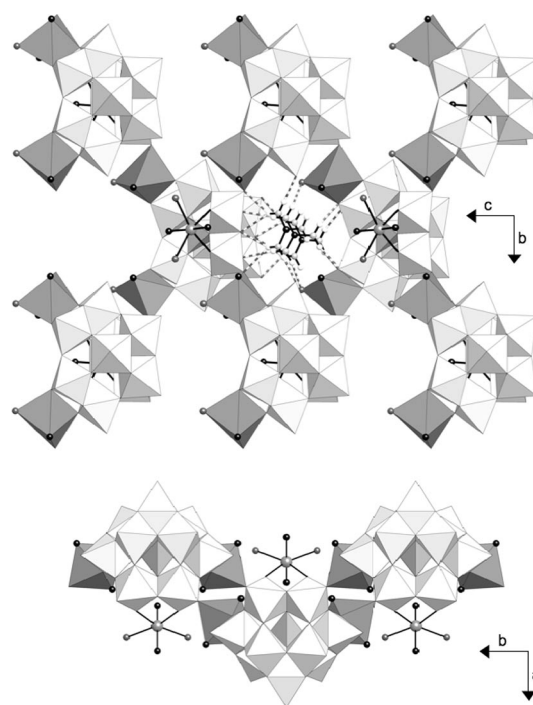


Figure 4. Top: Projection of the 2-dimensional arrangement of $[(CH_3)_2Sn(H_2O)_2]\{(CH_3)_2Sn(H_2O)\}_2(A-\alpha-PW_9O_{34})]^{3-}$ building blocks in **2** on the *bc* plane with a detail of the N–H⋯O_{POM} hydrogen-bonding network (dashed lines). Bottom: Side view along the *c* axis of a corrugated layer. Color code: same as Figure 2. Bridging Sn1 moieties represented as polyhedra to highlight the backbone of the hybrid layer. Hydrogen atoms omitted for clarity.

In the case of **3**, the three $\{(CH_3)_2Sn\}^{2+}$ electrophiles act as bridging moieties and they show *trans*-(CH₃)₂SnO₄ geometries analogous to the Sn1 centers in **2** but with significantly shorter Sn–O_w and Sn–O_t bonds (Table 1). Thus, each monomer is connected to six neighbors via six weak intermolecular Sn–O=W bridges, resulting in a chiral 3-dimensional architecture of tetrahedrally arranged building blocks that has been described previously in detail (Figure S3).^[3] It must be remembered that the discrete $[(CH_3)_2Sn(H_2O)]_{24}\{(CH_3)_2Sn\}_{12}(A-\alpha-PW_9O_{34})_{12}]^{36-}$ spherical cluster composed of twelve Sn–O=W bridged $\{(CH_3)_2Sn\}_3(A-\alpha-PW_9O_{34})$ building blocks was obtained under similar re-

action conditions when Cs^+ was used as crystallizing agent.^[3c] These results, together with the observation of a single ^{119}Sn -NMR signal for the reaction mixture of the dodecamer, constitute a strong indication that the 3:1 reaction of $\{(\text{CH}_3)_2\text{Sn}\}^{2+}$ with $[\text{A-}\alpha\text{-PW}_9\text{O}_{34}]^{9-}$ in water at acidic pH results in the monomeric $[\{(\text{CH}_3)_2\text{Sn}(\text{H}_2\text{O})_2\}_3(\text{A-}\alpha\text{-PW}_9\text{O}_{34})]^{3-}$ species of idealized C_{3v} symmetry (see Figure 3 for analogy). Furthermore, they illustrate the ability of this monomeric species to assemble in a versatile mode to form supramolecular architectures with features governed by key factors as the type of counteranion (extended with $[\text{C}(\text{NH}_2)_3]^+$ vs. discrete with Cs^+) or the pH for a given templating cation such as $[\text{C}(\text{NH}_2)_3]^+$ (2-dimensional at pH = 3.0 vs. 3-dimensional at pH = 2.0). Dissolution of **2** and **3** should proceed via the rupture of the very long Sn-O=W bridges and result in the monomers mentioned above, but the very low solubility of these compounds impeded us to obtain useful NMR results to ascertain this point (also ion exchange was impossible).

Conclusions

Our work illustrates the richness displayed by the chemistry of organotin-functionalized POMs. In the particular case of dimethyl-containing 9-phosphotungstates, the $[\text{C}(\text{NH}_2)_3]^+$ cation can be used as structure directing agent to isolate up to three different compounds from the 1 $[\text{A-}\alpha\text{-PW}_9\text{O}_{34}]^{9-}$: 3 $\{(\text{CH}_3)_2\text{Sn}\}^{2+}$ reaction with the pH as the single variable. The polyanion $[\{(\text{CH}_3)_2\text{Sn}(\text{H}_2\text{O})\}_3(\text{A-}\alpha\text{-PW}_9\text{O}_{34})]^{5-}$ in **1** is obtained at moderately acidic pH and it consists of a 1-dimensional arrangement of alternating $[\text{A-}\alpha\text{-PW}_9\text{O}_{34}]^{9-}$ subunits and *trans*-($\text{CH}_3)_2\text{SnO}_4$ bridging moieties. The monomeric $[\{(\text{CH}_3)_2\text{Sn}\}_3(\text{A-}\alpha\text{-PW}_9\text{O}_{34})]^{3-}$ species is formed at lower pH and its capability to assemble in a versatile mode via weak intermolecular Sn-O=W bridges results in two different $[\text{C}(\text{NH}_2)_3]^+$ templated architectures depending on the pH: the 2-dimensional **2** at pH = 3.0 and the 3-dimensional **3** at pH = 2.0.

Experimental Section

General Remarks: The precursor $\text{Na}_9[\text{A-}\alpha\text{-PW}_9\text{O}_{34}] \cdot 13\text{H}_2\text{O}$ was synthesized according to literature procedures and identified by infrared spectroscopy.^[7] All other chemicals were purchased from commercial sources and used without further purification. Elemental analyses were performed by Analytische Laboratorien, Lindlar, Germany. Infrared spectra were obtained as KBr pellets on a Nicolet Avatar 370 FT-IR spectrophotometer. Thermal analyses were carried out on a TA Instruments SDT Q600 thermobalance with a 100 mL/min flow of N_2 ; the temperature was ramped from 20 to 800 °C at a rate of 5 °C/min. All measurements were performed on crystalline samples, and each compound had an easily distinguishable crystal morphology (thin needles for **1**, rectangular blocks for **2**, and crystals with a tetrahedral shape in the case of **3**). Solid samples were carefully inspected under an optical microscope prior to use. This, together with repeated single-crystal X-ray diffraction measurements, did not show any evidence for a mixture of phases.

General Synthetic Procedure: To an aqueous (30 mL) solution of $(\text{CH}_3)_2\text{SnCl}_2$ (0.132 g, 0.60 mmol) powdered $\text{Na}_9[\text{A-}\alpha\text{-PW}_9\text{O}_{34}] \cdot 13\text{H}_2\text{O}$ (0.534 g, 0.20 mmol) was added. The pH of the resulting solution was adjusted to the desired value if necessary using aqueous 6 M HCl, and after heating to 80 °C for 30 min and cooling down to room temperature, a few drops of aqueous 1 M $[\text{C}(\text{NH}_2)_3]\text{Cl}$ (0.5 mL) were added. Colorless single-crystals suitable for X-ray diffraction were obtained by slow evaporation of the final solution at room temperature.

$\text{Na}_{0.5}[\text{C}(\text{NH}_2)_3]_{4.5}[\{(\text{CH}_3)_2\text{Sn}(\text{H}_2\text{O})\}_3(\text{A-}\alpha\text{-PW}_9\text{O}_{34})] \cdot 8.5\text{H}_2\text{O}$ (1**):** The initial pH of the solution was 4.5 and it was not modified before heating. A white precipitate of **1**, as indicated by IR spectroscopy, was formed overnight and it was filtered off. Needle-like crystals were obtained from the mother liquor after 2–3 weeks and they were isolated by filtration. Yield: 0.08 g of crystalline material (13% based on P). $\text{C}_{8.5}\text{H}_{58}\text{N}_{13.5}\text{Na}_{0.5}\text{O}_{43.5}\text{PSn}_3\text{W}_9$ (2980.1): calcd. C 3.43, H 1.96, N 6.34, Na 0.39, P 1.04, Sn 7.97, W 55.35; found C 4.06, H 2.05, N 6.23, Na 0.12, P 1.10, Sn 8.50, W 54.48. IR: $\tilde{\nu}$ = 1188 (w), 1082 (s), 1064 (s), 1007 (m), 934 (s), 904 (s), 891 (sh), 834 (s), 784 (vs), 718 (s), 668 (s), 595 (w), 571 (w), 518 (m) cm^{-1} .

$[\text{C}(\text{NH}_2)_3]_3[\{(\text{CH}_3)_2\text{Sn}(\text{H}_2\text{O})_2\}_2\{(\text{CH}_3)_2\text{Sn}(\text{H}_2\text{O})\}_2(\text{A-}\alpha\text{-PW}_9\text{O}_{34})] \cdot 8\text{H}_2\text{O}$ (2**):** The pH of the solution was adjusted to 3.0 by addition of aqueous 6 M HCl before heating. Block-like crystals were formed after ca. 1 week and they were isolated by filtration. Yield: 0.13 g of crystalline material (21% based on P). $\text{C}_9\text{H}_{60}\text{N}_9\text{O}_{46}\text{PSn}_3\text{W}_9$ (3072.4): calcd. C 3.52, H 1.97, N 4.10, P 1.01, Sn 11.59, W 53.86; found C 3.69, H 1.95, N 4.10, P 1.19, Sn 11.71, W 53.96. IR: $\tilde{\nu}$ = 1208 (w), 1075 (s), 1016 (m), 943 (s), 919 (s), 888 (m), 833 (s), 784 (vs), 721 (vs), 596 (w), 576 (w), 522 (m) cm^{-1} .

$\text{Na}[\text{C}(\text{NH}_2)_3]_2[\{(\text{CH}_3)_2\text{Sn}(\text{H}_2\text{O})\}_3(\text{A-}\alpha\text{-PW}_9\text{O}_{34})] \cdot 9\text{H}_2\text{O}$ (3**):** The specific synthesis of **3** (pH = 2) has been previously reported elsewhere.^[3j]

X-ray Crystallography: Crystallographic data for compounds **1** and **2** are summarized in Table 2. The crystal structure of **3** has been previously reported elsewhere.^[3j] Single crystals were mounted in Hampton cryoloops for indexing and intensity data collection at 173(2) K. Data were collected on a Bruker X8 APEX II CCD single-crystal diffractometer with κ geometry and graphite-monochro-

Table 2. Crystallographic data for compounds **1** and **2**.^[a]

	1	2
Formula	$\text{C}_{8.5}\text{H}_{58}\text{N}_{13.5}\text{Na}_{0.5}\text{O}_{43.5}\text{PSn}_3\text{W}_9$	$\text{C}_9\text{H}_{60}\text{N}_9\text{O}_{46}\text{PSn}_3\text{W}_9$
fw /g mol ⁻¹	2980.1	3072.4
Crystal system	tetragonal	orthorhombic
Space group	<i>I4</i>	<i>Pnma</i>
<i>a</i> /Å	29.9941(4)	25.0889(5)
<i>b</i> /Å	29.9941(4)	17.5925(4)
<i>c</i> /Å	13.3457(4)	12.8199(3)
<i>V</i> /Å ³	12006.4(4)	5658.4(2)
<i>Z</i>	8	4
$\rho_{\text{calcd.}}$ /g cm ⁻³	3.308	3.607
μ /mm ⁻¹	18.114	19.649
Reflections:		
collected	175926	260877
unique (<i>R</i> _{int})	12060 (0.112)	7540 (0.136)
observed (<i>I</i> > 2σ)	10447	6318
Parameters	333	206
<i>R</i> (<i>F</i>) (<i>I</i> > 2σ)	0.041	0.046
<i>wR</i> (<i>F</i> ²) (all data)	0.097	0.129
GoF	1.044	1.007
Flack parameter	−0.008(11)	

$$[a] \quad R(F) = \frac{\sum |F_o| - |F_c|}{\sum |F_o|}; \quad wR(F^2) = \frac{\{\sum [w(F_o^2 - F_c^2)^2]\}}{\sum [w(F_o^2)^2]}^{1/2}.$$

mated Mo- K_{α} radiation ($\lambda = 0.71073 \text{ \AA}$). Data collections, unit cell determinations, intensity data integrations, routine corrections for Lorentz and polarization effects, and multi-scan absorption corrections were performed using the APEX2 software package.^[8] The structures were solved and refined using the SHELXTL software package.^[9] Direct methods were used to solve the structures and to locate the heavy atoms. The remaining atoms were found from successive Fourier syntheses. Heavy atoms (W, Sn) were refined anisotropically. Lighter atoms (C, O and N) were refined isotropically. Hydrogen atoms of the methyl groups and the guanidinium cations were placed in calculated positions and refined with a riding model using standard SHELXL parameters. The final geometrical calculations were carried out with the PLATON program.^[10]

CCDC-757618 (for **1**) and -757619 (for **2**) contain the supplementary crystallographic data for this paper. These data can be obtained free of charge from The Cambridge Crystallographic Data Centre via www.ccdc.cam.ac.uk/data_request/cif.

Supporting Information (see also the footnote on the first page of this article): FT-IR spectra (Figure S1) and TGA curves (Figure S2) for **1–3**. Detailed crystal packing of **3** viewed along the [111] direction (Figure S3).

Acknowledgments

U. K. thanks Jacobs University and the Fonds der Chemischen Industrie for financial support. S. R. thanks Gobierno Vasco/Eusko Jaurlaritza for his postdoctoral fellowship. We thank Dr. M. H. Dickman for help with XRD.

- [1] a) M. T. Pope, *Heteropoly and Isopoly Oxometalates*, Springer-Verlag, Berlin, Germany, **1983**; b) M. T. Pope, A. Müller, *Angew. Chem. Int. Ed. Engl.* **1991**, *30*, 34–48; c) *Polyoxometalates: From Platonic Solids to Antiretroviral Activity* (Eds.: M. T. Pope, A. Müller), Kluwer, Dordrecht, The Netherlands, **1994**; d) *Chem. Rev.* **1998**, *98*, special thematic issue; e) *Polyoxometalate Chemistry: From Topology via self-Assembly to Applications* (Eds.: M. T. Pope, A. Müller), Kluwer, Dordrecht, The Netherlands, **2001**; f) *Polyoxometalate Chemistry for Nanocomposite Design* (Eds.: M. T. Pope, T. Yamase), Kluwer, Dordrecht, The Netherlands, **2002**; g) *Polyoxometalate Molecular Science* (Eds.: J. J. Borrás-Almenar, E. Coronado, A. Müller, M. T. Pope), Kluwer, Dordrecht, The Netherlands, **2003**; h) M. T. Pope, in: *Comprehensive Coordination Chemistry II* (Eds.: J. A. McCleverty, T. J. Meyer), Elsevier Ltd., Oxford, UK, **2004**; i) *Eur. J. Inorg. Chem.* **2009**, issue 34 (dedicated to Polyoxometalates; Guest Ed.: U. Kortz).
- [2] For some recent examples, see: a) G. Szani, M. T. Pope, *Dalton Trans.* **2004**, 1989–1994; b) F. Hussain, U. Kortz, R. J. Clark, *Inorg. Chem.* **2004**, *43*, 3237–3241; c) S. Bareyt, S. Piligkos, B. Hasenknopf, P. Gouzerh, E. Lacôte, S. Thorimbert, M. Malacria, *J. Am. Chem. Soc.* **2005**, *127*, 6788–6794; d) N. Belai, M. T. Pope, *Polyhedron* **2006**, *25*, 2015–2020; e) K. Micoine, B. Hasenknopf, S. Thorimbert, E. Lacôte, M. Malacria, *Org. Lett.* **2007**, *9*, 3981–3984; f) S. Reinoso, M. H. Dickman, A. Praetorius, L. F. Piedra-Garza, U. Kortz, *Inorg. Chem.* **2008**, *47*, 8798–8806; g) C. Boglio, K. Micoine, E. Derat, R. Thouvenot, B. Hasenknopf, S. Thorimbert, E. Lacôte, M. Malacria, *J. Am. Chem. Soc.* **2008**, *130*, 4553–4561; h) K. Micoine, B. Hasenknopf, S. Thorimbert, E. Lacôte, M. Malacria, *Angew. Chem. Int. Ed.* **2009**, *48*, 3466–3468; i) S. Reinoso, L. F. Piedra-Garza, M. H. Dickman, A. Praetorius, M. Biesemans, R. Willem, U. Kortz, *Dalton Trans.* **2010**, 248–255.
- [3] a) F. Hussain, M. Reicke, U. Kortz, *Eur. J. Inorg. Chem.* **2004**, 2733–2738; b) F. Hussain, U. Kortz, *Chem. Commun.* **2005**, 1191–1193; c) U. Kortz, F. Hussain, M. Reicke, *Angew. Chem. Int. Ed.* **2005**, *44*, 3773–3777; d) F. Hussain, U. Kortz, B. Keita, L. Nadjo, M. T. Pope, *Inorg. Chem.* **2006**, *45*, 761–766; e) S. Reinoso, M. H. Dickman, M. Reicke, U. Kortz, *Inorg. Chem.* **2006**, *45*, 9014–9019; f) S. Reinoso, M. H. Dickman, U. Kortz, *Inorg. Chem.* **2006**, *45*, 10422–10424; g) F. Hussain, M. H. Dickman, U. Kortz, B. Keita, L. Nadjo, G. A. Khitrov, A. G. Marshall, *J. Cluster Sci.* **2007**, *18*, 173–191; h) S. Reinoso, M. H. Dickman, M. F. Matei, U. Kortz, *Inorg. Chem.* **2007**, *46*, 4383–4385; i) S. Reinoso, M. H. Dickman, U. Kortz, *Eur. J. Inorg. Chem.* **2009**, 947–953; j) L. F. Piedra-Garza, S. Reinoso, M. H. Dickman, M. M. Sanguineti, U. Kortz, *Dalton Trans.* **2009**, 6231–6231.
- [4] See, for example: a) D.-L. Long, P. Kögerler, L. J. Farrugia, L. Cronin, *Angew. Chem. Int. Ed.* **2003**, *42*, 4180–4183; b) C. Streb, D.-L. Long, L. Cronin, *CrystEngComm* **2006**, *8*, 629–634; c) D.-L. Long, E. Burkholder, L. Cronin, *Chem. Soc. Rev.* **2007**, *36*, 105–121.
- [5] K. Nakamoto, *Infrared and Raman Spectra of Inorganic and Coordination Compounds*, Wiley Interscience, New York, USA, **1997**.
- [6] I. D. Brown, D. Altermatt, *Acta Crystallogr., Sect. B* **1985**, *41*, 244–247.
- [7] P. J. Domaille, *Inorg. Synth.* **1990**, *27*, 100.
- [8] APEX2, version 2.1-0, Bruker AXS Inc., Madison, Wisconsin, USA, **2005**.
- [9] G. M. Sheldrick, *Acta Crystallogr., Sect. A* **2008**, *64*, 112–122.
- [10] A. L. Spek, *PLATON*, Utrecht Universiteit, Utrecht, The Netherlands, **2005**.

Received: February 16, 2010
Published Online: May 5, 2010